Co-published by
Institute of Fluid-Flow Machinery
Polish Academy of Sciences
Committee on Thermodynamics and Combustion
Polish Academy of Sciences

http://www.imp.gda.pl/archives-of-thermodynamics/

A holistic approach to the total energy and cost for carbon capture and sequestration

Efstathios E. Michaelides[a]

[a]Department of Engineering, Texas Christian University, Fort Worth, TX, 76129, USA, e-mail: e.michaelides@tcu.edu

Received: 14.09.2023; revised: 12.01.2024; accepted: 15.01.2024

Abstract

Carbon capture and sequestration from a stationary source comprises four distinct engineering processes: separation of CO_2 from the other flue gases, compression, transportation, and injection into the chosen storage site. An analysis of the thermodynamic and transport properties of CO_2 shows that dissolving this gas in seawater at depths more than 600 m is, most likely, an optimal long-term storage method; and that for transportation, the CO_2 must be in the denser supercritical state at pressures higher than 7.377 MPa. The separation, compression, transportation, and injection processes require significant energy expenditures, which are determined in this paper using realistic equipment efficiencies, for the cases of two currently in operation coal power plants in Texas. The computations show that the total energy requirements for carbon removal and sequestration are substantial, close to one-third of the energy currently generated by the two power plants. The cost analysis shows that two parameters – the unit cost of the pipeline and the discount factor of the corporation – have a very significant effect on the annualized cost of the CCS process. Doubling the unit cost of the pipeline increases the total annualized cost of the entire CCS project by 36% and increasing the discount rate from 5% to 15% increases this annualized cost by 32%.

Keywords: Carbon capture; Carbon sequestration; Minimum work; CO_2 removal; Cost of carbon sequestration.

Vol. 45(2024), No. 1, 5–16; doi: 10.24425/ather.2024.150433

Cite this manuscript as: Michaelides, E.E. (2024). A holistic approach to the total energy and cost for carbon capture and sequestration. *Archives of Thermodynamics*, 45(1), 5–16.

1. Introduction

Carbon capture and storage (CCS) is considered one of the ways to reduce the global carbon dioxide atmospheric emissions by safely storing this greenhouse gas. CCS entails a series of processes that include a) separation of the CO_2 gas from the combustion effluent mixture; b) compression to achieve a dense state for transportation; c) transportation of the gas in a dense phase to the storage facility; and d) long-term storage, monitoring and prevention of CO_2 from entering the atmosphere.

Major point sources, for which CCS is proposed, include fossil fuel power plants (coal as well as gas-fired); cement production factories; and syngas production plants. These stationary, large point sources accounted for 49% of the total global CO_2 emissions in 2020 [1]. The capture and sequestration of a large fraction of these emissions will result in a substantial decrease of the CO_2 accumulation in the atmosphere. The transportation sector (the exhausts of moving vehicles), which contributes to 27% of the global CO_2 emissions, is not targeted for CCS be-

Nomenclature

D – diameter, m
f – friction factor
g – gravitational acceleration, m^2/s
h – enthalpy, kJ/kg
L – length scale, m
P – pressure, kPa
Re – Reynolds number, $= Dv\rho/\mu$
T – temperature, K
t – time, s
V – velocity, m/s
w – specific work, kJ/kg
W – power, kW

Greek symbols

η – efficiency
μ – dynamic viscosity, Pa·s
ρ – density, kg/m^3

Subscripts and Superscripts

0 – (sub) environment condition
0 – (sup) ideal, reversible
a – air
g – gas
n – time step number
sep – separation
T – terminal
w – water

cause emissions from this sector are diffuse, and capture is not practical in vehicles in motion.

An early Intergovernmental Panel for Climate Change (IPCC) report [2] suggested as candidate locations for CO_2 storage tight geological formations – oil and gas fields, un-minable coal beds, and deep saline aquifers – and offshore, deep ocean storage, where the CO_2 is injected at a substantial depth into the seawater. Another suggestion is industrial fixation of this greenhouse gas into solid inorganic carbonates accompanied by local disposal [2, 3]. However, this method requires very large amounts of other chemicals and very high additional energy for the mining and transportation of the chemicals to the disposal sites. For example, the calcination and sequestration of one ton of CO_2 requires 1.27 tons of CaO, or 1.68 tons of $Ca(OH)_2$ to be mined and transported to the source of CO_2.

Several chemical separation processes have been developed for the removal of CO_2 from the combustion products mixture. Among the chemical processes for large-scale CO_2 capture, separation with ammonia and amines appears to be the most promising. Rao and Rubin [4] devised methods to improve the capture efficiency with amines. Valenti et al. [5] performed a detailed study on the chemical separation and capture of CO_2 using chilled ammonia. An analytical/numerical study using ammonia by Bonalumi et al. [6] includes some of the economic aspects and estimated that CO_2 separation using ammonia will cause significant electricity generation costs, close to $124/MWh – three to four times higher than the wholesale electricity price in most States of the USA.

Separation of CO_2 with amine absorption and subsequent regeneration of the amine has received a great deal of attention. Weiland et al. proposed the use of a solution of monoethanolamine (MEA) and methyldiethanolamine (MDEA) for the separation of CO_2 from the other gases [7]. Aqueous MEA and piperazine as CO_2 removal solvents, were extensively studied by Aliyon et al. [8]. Carapellucci et al. [9] also considered the MEA capture in the retrofitting of a coal-fired power plant with a molten carbonate fuel cell, which concentrates the CO_2 gas in its anode and simplifies its capture. Other amine solutions were studied by several researchers, including Rochelle et al. [10] and Li et al. [11]. The latter included calculations of the energy requirements for the CO_2 separation and capture using several amine-based solvents. Among the studies on the chemical separation methods, Furcasa et al. advocated the use of the carbonate mineral *trona* (trisodium hydrogendicarbonate dihydrate) as the main sorbent feedstock source [12]. A comparison of the environmental and ecological impacts using ammonia and amines for CO_2 capture as well as life-cycle assessments were conducted by Strube et al. [13], who concluded that such impacts are significantly less in the long run if amines are used.

Several studies considered the performance of chemical separation methods of CO_2 from the combustion effluents within the framework of specific power plants. Lee et al. [14], considered the CO_2 capture in a 300 MW Integrated Gas Combined Cycle (IGCC) using MDEA and a *Solexol* chemical processes. Their exergy analysis pointed ways to improve the separation processes, which have very low exergetic efficiency. Other separation studies with IGCC cycles that considered chemical separation methods are those by Kunze et al. [15] who used methanol as the chemical agent for capture; Arabkhalaj et al. [16] who compared the effects of two coal types (low-ash and high-ash) in the gas separation process; and the analytical, thermos-economics study by Rosner et al. [17]. An exergo-environmental analysis of CO_2 removal by chemicals including the regeneration process by Petrakopoulou et al. highlighted the environmental advantages of the chemical processes, but also showed the substantial amount of heat input at relatively high temperatures, for the regeneration of the chemicals [18]. A recent review article by Akinola et al. [19] summarizes absorbent materials for the post-combustion capture of CO_2 and details the molecular simulation processes that characterize the absorption of this gas.

A second category of separation methods for CO_2 removal from the flue gases is mechanical separation methods, using primarily membranes. Zhang et al. [20] determined that the selectivity of current-technology membranes is in the range of 70–90% and that high amounts of energy need to be expended for the flue gas pressurization – a significant constraint for the membrane separation technology. In order to supplement the energy consumed by the separation processes, Li et al. [2] suggested that a solar-assisted cycle be used for the capture of CO_2, while Carapellucci et al. [22] suggested a biomass-assisted process. A review of the solar-assisted coal cycles by Saghafifar

and Sabra [23] advised that solar systems composed of large solar collectors be used to supply the high-temperature heat for the chemical separation, in order to avoid the deterioration in the power plant's efficiency. This would entail additional capital cost and exergy dissipation emanating from the conversion of the solar irradiance to heat [24].

A number of recent studies examined the application of CCS technology in specific industries that are heavily dependent on fossil fuels. The removal of CO_2 enables these energy-intensive industries to operate in their traditional ways, while contributing to the mitigation of Global Climate Change. Among these, Paltsev et al. performed a computational study on CCS in "hard to abate sectors" of industry that include cement, chemicals, and the steel industries [25]. Lee et al., used a hybrid economic model to examine the application of CCS in the steel industry [26]. Al Baradi et al. conducted a review of the CO_2 shipping methods in order to extend the carbon abatement to countries and industries where CCS is not feasible, because of their geographic location [27].

In order to answer the question of the minimum equivalent mechanical work required for the separation of CO_2 from other gases (in this case the atmosphere or flue gases), Michaelides [28] used the classical concept of reversible semipermeable membranes – a concept readily used in Thermodynamics – and determined the minimum work required for the separation, regardless of the separation method (chemical, electrochemical, mechanical, etc.). This minimum work is the benchmark of the separation processes and helps define realistic efficiencies for these processes.

After separation, the CO_2 gas must be compressed and transported to the storage sites, which are located at long distances from the generation/capture sites. To minimize pressure losses, compression to supercritical states is recommended. This mode of transportation was examined by Zai et al. [29], who also calculated the water requirements for the pressurization and transportation as well as some commercial uses of the captured CO_2. Geological studies on the storage of CO_2, primarily appraise the suitability of geological formations for the long-term sequestration of CO_2 at supercritical conditions, as for example, in the Utsira formation [30] off the coast of Norway; in several sites considered in Japan [31]; in the pilot-study in the Frio location in Texas [32]; and in the deep sea [33]. Regarding deep ocean sequestration, Caldeira and Wicket [34] warned about the environmental risks of hydrate formation and ocean acidification resulting from the disposal of large CO_2 quantities; and in another study [35] about the possible exchange of this gas between the ocean and the atmosphere.

While CCS entails several technological processes, most of the studies on CCS only consider one aspect of these processes, primarily the separation of this greenhouse gas. This paper contributes to the body of knowledge by presenting a holistic energy analysis of the entire CCS sequence of processes. Some of the novel parts of this paper include: the separation and capture efficiencies, based on the minimum work benchmark; the power for the compression and transportation of CO_2 in real-size pipelines; the analysis of the injection depth and the determination of the maximum size of bubbles for the injection of the CO_2 in the ocean. Based on the thermodynamic properties and the volume of the produced CO_2, the paper shows that deep ocean injection is a realistic storage location for the long run. The energy and power requirements of all the CCS processes are analyzed and the effect of the CCS on the power generated by two power plants currently in operation is determined. In addition to the energy requirements, this study presents the monetary cost for the entire CCS using realistic parameters from two coal power plants, currently in operation. This economic analysis shows the effects of the entire CCS process on the net electric power generated by the power plants, their overall efficiency, and the cost of electricity generated. In summary, this study offers a holistic view of the energy and monetary requirements for CCS to become a realistic solution to the global climate change.

2. Relevant properties of CO_2

2.1. Thermodynamic properties

At ambient conditions (0.1 MPa and 300 K) CO_2 is a gas, usually modelled as an ideal gas. The critical temperature of CO_2 is 304.13 K (31.0°C) and its critical pressure is 7.377 MPa, which implies that CO_2 may turn to the dense supercritical state at ambient temperatures. The dense states of this material (liquid or supercritical) are essential for its transportation, where pressure losses must be kept low. Fig. 1 depicts the T,s diagram of CO_2, with data obtained from [36]. Four isobars at 6, 8, 10 and 12 MPa are depicted in the figure.

While it is possible to transport CO_2 in the liquid state at lower than critical pressures, when the ambient temperature

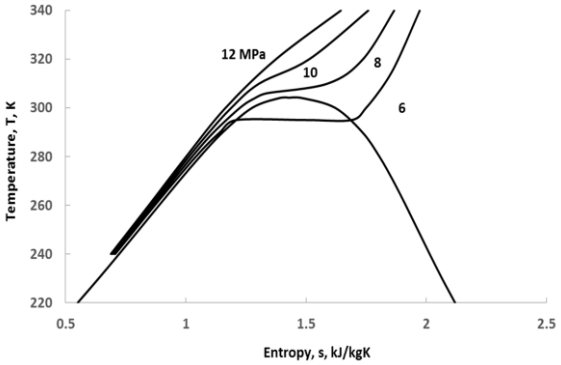

Fig. 1. T,s diagram of carbon dioxide with four isobars around the critical point.

rises (e.g. on summer days) vapour bubbles are formed in the pipeline, the flow becomes two-phase flow, the average velocity increases, and the pressure loss significantly rises. In addition, the risk for pipeline erosion increases. Because of this, the long-distance CO_2 transportation is always recommended at supercritical pressures.

An important consideration for the long-distance transportation of all fluids is the minimization of frictional power dissipation, which is proportional to the third power of the transport velocity, *V*. This is achieved in practice with wider pipelines and high densities of the transported fluid. Fig. 2 shows the density

of carbon dioxide as a function of the local pressure for four isotherms (at 273 K, 290 K, 300 K and 310 K). Because the CO_2 pipelines are typically buried underground, at depths more than 1 m, extreme air temperatures are avoided, and the four temperatures represent pipeline conditions for all seasons. The four isotherms show that at supercritical pressures – in particular, above 10 MPa – the transported fluid is at sufficiently high densities, which result in lower velocities and friction dissipation. This is the practice in most existing CO_2 pipelines (e.g., for enhanced oil recovery applications) where the fluid typically enters at pressures higher than 10 MPa [37].

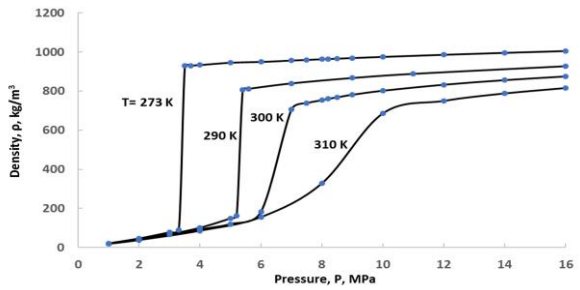

Fig. 2. Pressure density diagram with four isotherms for carbon dioxide.

2.2. Transport and storage properties

As it happens with all the substances in the vicinity of their critical points, the dynamic viscosity of CO_2 significantly varies with temperature and pressure. At any temperature close to the critical point, the dynamic viscosity of any substance is bound to be between the viscosity of the liquid and the viscosity of the vapor. At the typical transportation conditions $273 < T < 310$ K, $8 < P < 14$ MPa, the dynamic viscosity of CO_2 is in the range $10 \times 10^{-6} < \mu < 18 \times 10^{-6}$ Pa·s [38, 39]. It is of interest that the viscosity of CO_2 at these conditions is significantly lower than that of liquid water.

The CO_2 readily dissolves in water as well as in saline water. The solubility of CO_2 in water at 20 °C and 1 bar is 1.69 kg/m^3, and this value becomes significantly higher at higher pressures [40]. An interesting property of the saline water–CO_2 solution is that its density is slightly higher than that of saline water. For example, the seawater density at 4 MPa and 276.15 K increases from 1 031 kg/m^3 to 1 048 kg/m^3 at 6% CO_2 by mass as determined by Song et al. [41]. This characteristic is helpful for CO_2 sequestration, because the heavier solution of seawater–CO_2 sinks and settles at the bottom of the ocean instead of rising to the surface, where the CO_2 may escape into the atmosphere. The timescale of dissolved CO_2 in seawater is on the order of 500 years [42].

3. Mechanical work for CO_2 capture

Classical thermodynamics proves that the minimum work for the separation of CO_2 from a mixture of other gases is achieved with reversible semipermeable membranes [28]. When the CO_2 is separated from the mixture, its partial pressure increases from P_i to P_0=1 atm and the ideal (minimum) specific work w^0_{sep} for the separation is:

$$w^0_{sep} = T_0 R \ln\left(\frac{P_i}{P_0}\right) \approx T_0 R \ln(x_i), \quad (1)$$

where T_0 is the temperature at which separation occurs, typically the ambient; and R is the gas constant of CO_2, 0.189 kJ/kgK. Since CO_2 behaves as an ideal gas at low pressures the ratio of the pressures, P_i/P_0, is equal to the molar fraction of the gas, x_i, in the original mixture. Because $x_i < 1$, $w^0_{sep} < 0$ signifying that mechanical work needs to be spent for the separation of a gas from a mixture of other gases. The ideal separation work is 107 kJ/kg when the volume concentration of CO_2 is 0.15 – the typical concentration of flue gases – and becomes higher at lower concentrations. Eq. (1) also proves that the work for the separation of CO_2 from the flue gas mixture of a stationary CO_2 source (power plant, cement factory, etc. where $x_i \approx 0.15$) would be 3.5 times lower than the work to remove this gas from the atmosphere (where $x_i \approx 0.0004$). Such considerations favour the separation and removal of CO_2 at the point sources where its concentration is significantly higher than in the atmosphere.

Reversible semipermeable membranes that would efficiently separate the CO_2 from a gaseous mixture have not been developed. The practical methods for CO_2 separation are characterized by an efficiency, defined as the ratio of the ideal specific work from Eq. (1) to the actual specific work spent for the separation:

$$\eta_{sep} = \frac{w^0_{sep}}{w_{act}}, \quad (2)$$

at the current state of technology, the separation efficiencies are rather low, when compared to the minimum work benchmark of Eq. (1). Actual mechanical membranes that operate in several stages at high pressures, have rather low selectivity and their efficiency is below 10% [20]. Liquefaction and separation of CO_2 entails the pressurization of the entire original gaseous mixture and subsequent throttling for the removal of CO_2 droplets, and its efficiencies are in the range of 5−8% [24]. Chemical methods for the separation, e.g. using ammonia or amines, entail mechanical (parasitic) work for the flow of the gas and the chemicals as well as heat at a relatively high temperature, 81−115 °C. When the equivalent work of the heat is added to the parasitic work, the efficiencies of the chemical methods are in the range of 8−13% [43, 16, 5]. This is in line with the observations in the original IPCC report [2] and by Davison [44] that the CO_2 capture alone reduces the overall efficiency of a power plant by 6−11% points and that, depending on the type of power plant, 11−25% more fuel is required for the capture process per MWh of electricity generated. If the parasitic mechanical work is minimized or eliminated – e.g., using gravitational rather than mechanical separation of the CO_2-rich amines with phase-change solvents [45] – the efficiency of the separation process may slightly improve to be in the range of 15−20%.

4. Mechanical work for compression and transportation

It is observed in the T,s diagram of Fig. 1 that, at relatively low pressures and ambient temperatures, CO_2 exists as a two-phase mixture. Two-phase flow is avoided in long-distance pipelines because of two detrimental effects:

a) the low density of the vapour dramatically increases the local velocity and the power dissipation, sometimes leading to pipeline chocking (critical flow) [46], and
b) vapour bubbles and slugs cause vibrations that damage the pipelines.

The liquefaction and transportation of CO_2 at low temperatures in the liquid phase presents significant technological difficulties and batch transportation by trucks or railways is very expensive. Such considerations leave pipeline transportation in the supercritical state as the only mode for the long-distance transportation of CO_2. The existing CO_2 pipelines for enhanced oil recovery and smaller pilot pipelines, which extend to more than 2 500 km in the USA, follow this practice too [2, 37]. Before transportation in these pipelines, chemical scrubbers remove the small amounts of hydrogen sulfide, and sulfur oxides as well as the traces of other corrosive materials that were not separated from the CO_2 stream. If such corrosive materials are not removed, the interior of the pipelines must be covered by a corrosion-resistant lining.

While the theory of elementary thermodynamics proves that isothermal compression is the optimum method of pressurization, such processes entail heat transfer and are extremely slow to be used for practical applications. Instead, industrial compressors (which ideally operate isentropically) with intercoolers, in two to four compression stages pressurize the gas. The actual power required for the compressors in a multistage compression unit is:

$$\dot{W}_{pr}^{act} = \dot{m}\left(\frac{1}{\eta_{C1}}\Delta h_{s1} + \frac{1}{\eta_{C2}}\Delta h_{s2} + \frac{1}{\eta_{C3}}\Delta h_{s3} + \ldots\right), \qquad (3)$$

where Δh_{si} and η_{Ci} represent the isentropic enthalpy difference and the corresponding isentropic efficiency of each compressor and the sum is extended to the number of stages. The efficiency of large industrial compressors is in the range of 75−85%. The small parasitic power for the operation of the intercoolers may be incorporated in the efficiencies η_{Ci}.

The mechanical energy equation for the transportation of a fluid from point 1 to point 2 in a pipeline is [47]:

$$P_1 + \rho g z_1 + \frac{1}{2}\rho V_1^2 + \frac{|\dot{W}_{tr}^0|\rho}{\dot{m}} = P_2 + \rho g z_2 + \frac{1}{2}\rho V_2^2 + \frac{1}{2}\rho V_{av}^2\left(f\frac{L}{D} + \sum K_{ml}\right), \qquad (4)$$

where V_{av} is the average velocity of the fluid in the pipeline; P is the static pressure; ρ is the density of the fluid; g is the gravitational constant; $\dot{W}_{tr}^0$ is the pumping power needed for the transportation; $\dot{m}$ is the mass flow rate of the fluid; D is the diameter of the pipe; f is the friction factor of the pipe; L is the pipeline length between points 1 and 2; and K_{ml} represents the so-called "minor losses" in the pipeline that include elbows, other bends, safety valves, etc. The last term essentially represents the energy dissipation in the pipeline and becomes the dominant term in long-distance transportation, where the length is on the order of 100−1 000 km. In most of the existing CO_2 pipelines, the initial gas compression (in the range of 10−15 MPa) at the starting point of the pipeline is sufficient to overcome the dissipation during transportation, and for the gas to arrive at point 2 at supercritical pressure and low density. In this case, $\dot{W}_{tr}^0 = 0$. If this is not the case, intermediate compression stations must be built from an intermediate point i to point 2, to supply additional power. The actual power needed for the transportation of any fluid in the segment 1–2 of a pipeline becomes [47]:

$$\dot{W}_{act}^{tr} = \frac{\pi}{8}D^2\rho V_{av}^3\left(f\frac{L}{D} + \sum K_{ml} + 2g\frac{z_2 - z_1}{V_{av}^2}\right), \qquad (5)$$

4.1. Effect of temperature

The ambient temperature significantly affects the density of a fluid in the vicinity of the critical point. The effect of ambient temperature on pipelines is shown in Fig. 3, which depicts the pressure loss and power dissipation for a horizontal pipeline carrying 300 kg/s (approximately the average mass flow rate generated in a 620 MW power plant) of CO_2, for a length of 500 km. The two pipelines considered for this transportation are schedule-30 steel pipes with nominal diameters of 24 inch (ID = 581 mm) and 30-inch (ID = 730 mm). Schedule 30 corresponds to steel pipelines with sufficient thickness (0.562" or 14.3 mm and 0.625" or 15.9 mm) to withstand the high internal pressure of the supercritical fluid. Such pipelines have sufficient peripheral area for the heat generated from the frictional power dissipation to be transferred to the surroundings. As a result, they operate isothermally and constant CO_2 temperature was assumed along the length of the pipeline, as specified in the ordinate of the figure. The pressure drop and power dissipation due to friction were calculated for a horizontal pipeline with zero minor losses using Eqs. (4) and (5) and a finite difference numerical scheme with segments of 5 km length. It is observed in Fig. 3 that, when the ambient temperature rises above 308 K (35°C), both the dissipated power and the pressure drop increase substantially. To keep the pressure drop and the dissipation within the design conditions, the currently operating CO_2 pipelines in Texas are buried in the ground, at depths of at least 1 m, where the annual temperature variability is limited [2].

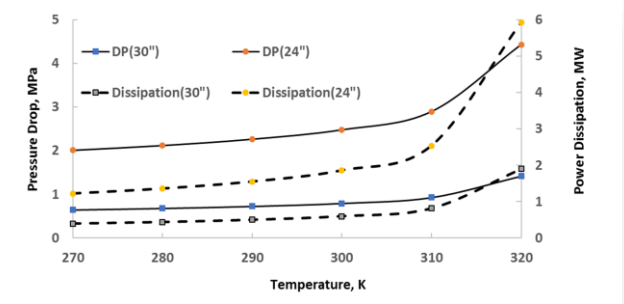

Fig. 3. Pressure drop and power dissipation in two pipelines carrying 300 kg/s of CO_2 for 500 km.

5. Storage locations – injection in oceans

Although the science of CO_2 capture and transportation has offered quantitative results and conclusions that may be followed with certainty, there are several non-technical and legal issues that will need to be resolved before many additional permits are issued for the large-scale and long-term storage of this gas. Among these issues are:

1. Lack of national and regional legal frameworks for the development of a CCS infrastructure. This includes rights-of-way for the transportation pipelines.
2. The need for significant economic incentives (a national carbon tax or emissions allowances), which are lacking in most countries.
3. The legal custody (stewardship) of the stored CO_2. Who is responsible for any atmospheric leakages of the stored CO_2, and the monitoring of the storage sites?
4. For international conventions and agreements should CCS be treated as a reduction of emissions or as removal from the atmosphere?

With the current emphasis on decarbonization, it is reasonable to assume that these economic and legal issues will be resolved at the national and international levels. Then the selection of storage sites will become of importance. CO_2 storage may take place onshore, in geological formations – coal mines, deep saline aquifers, oil fields, etc. – and offshore.

Regarding inland storage, it must be noted that, for any meaningful impact on the global emissions, the CO_2 volume to be stored is very high and inland storage is hampered by the high temperature of the underground locations. If CO_2 were to be compressed to the supercritical pressure of 12 MPa and stored in underground mines and aquifers where the temperature is close to 50°C, the density of CO_2 would be 587 kg/m^3 [36]. Given that the total global emissions of CO_2 in 2021 amounted to 37.9×10^{12} kg [48], this corresponds to a volume of 64.6×10^9 m^3, or 406.1×10^9 bbl. In the same year, the total global volume of petroleum extraction from all the oil fields was 32.8×10^9 bbl, and this implies that, if all the oil fields in the world were used for CO_2 storage, only 8.1% of the emitted CO_2 could be stored in the depleted oil reservoirs. In the state of Texas, where CO_2 is extensively used for enhanced oil recovery, a single coal power plant (the Martin Lake plant, see section 6) generates enough CO_2 annually to fill 13% of the operational oil wells in the entire State.

A second problem with the onshore storage of CO_2 is that – since supercritical CO_2 is a powerful solvent, its molecule is planar and forms a weak acid with water – in the long run the action of the acid will induce cracks and passages that will allow the gas to escape from onshore geological formations that may have trapped methane (a three-dimensional molecule, which is inert with water) or other hydrocarbons. This was the conclusion of several geological studies on pilot CCS projects: The monitoring of a CO_2 injection facility in Frio, Texas, showed that CO_2 in saline aquifers decreases the brine pH and dissolves iron and carbonate oxyhydroxides. This weakens the surrounding rocks, allows CO_2 to escape via the induced cracks and may mobilize toxic metals and organic compounds, which have a path to migrate into the potable groundwater [32]. Another geological monitoring study in Cranfield, Mississippi revealed that the currently available models and computational tools do not yield sufficiently accurate predictions for the long-term fate and transport of CO_2 in aquatic reservoirs [49]. Given such uncertainties and the risk of catastrophic environmental impacts, it is doubtful that many permits will be issued for the long-term onshore storage of CO_2, including storage in aquifers.

5.1 Deep ocean injection

Offshore storage is different because the CO_2 readily dissolves in seawater and forms a mixture with higher density than the seawater [41]. The heavier CO_2 solution in saline water sinks to the bottom of the ocean, where it resides at very high hydrostatic pressure. In addition to the high pressures at the bottom of the ocean, the prevailing temperature of approximately 4°C reduces the chemical activity of the CO_2 molecules. The already-in-operation CCS facility in Sleipner West (Norway) is an offshore storage facility, where the CO_2 is injected in the sandstone of the Utsira formation (a Miocene era formation) at depths more than 1 000 from the surface of the sea [50]. The seawater and sediment column combine to keep the seawater–CO_2 mixture at high pressure, isolated, and chemically stable. Ozaki et al. [33] envisioned CO_2 disposal in the deep ocean by a fleet of ships in motion and high-pressure injection. The deep ocean sequestration of CO_2 is significantly less risky than onshore storage and is the preferable long-term storage location for the gas [2, 51].

For the CO_2 to dissolve in seawater, it must be injected as small bubbles/droplets and this is achieved with high-pressure atomizers – e.g., orifice, pressure swirl, spinning disk, and rotary atomizers – that will, typically, disperse the CO_2 in small droplets of sizes on the order of mm [52]. To facilitate injection, the transportation pipeline must be divided into multiple branches with small nozzles and atomizers that inject the drops of CO_2 in the ocean. Since the prevailing temperature in deep water is 277 K and the pressure at 600 m is 6.033 MPa, the CO_2 is liquid, and the small drops rise with terminal velocity [53]:

$$V_T = \frac{2(\rho_w - \rho_g) g \alpha^2}{9 \mu_w}, \tag{6}$$

where ρ_w and ρ_g are the densities of the seawater and the liquid CO_2; α is the radius of the drops; and μ_w is the viscosity of the seawater, approximately 0.00167 Ns/m^2. As the liquid droplets rise in the seawater, the CO_2 is slowly dissolved, the droplet size decreases and the terminal velocity decreases. The time scale for the mass transfer process from gaseous CO_2 in the seawater is [53]:

$$\tau_m = \frac{\alpha^2}{D}, \tag{7}$$

where D is the diffusion coefficient of CO_2 in the seawater, 1.6×10^{-9} m^2/s [54, 55]. Therefore, the length scale for the diffusion of the rising CO_2 drops is:

$$L_m = \frac{2(\rho_w - \rho_g) g \alpha^4}{9 \mu_w D}, \tag{8}$$

Figure 4 depicts the diffusion length scale of CO_2 in seawater. As the CO_2 diffuses into the seawater and the drops become smaller, the diffusion length-scale diminishes to a vanishing point, when all the CO_2 has been dissolved. Because of this, a distance of two length scales ($2L_m$) is sufficient for the complete dissolution of this gas in seawater. A glance at Fig. 4 proves that, if the CO_2 is injected at 500–600 m depth all the droplets up to 2.6 mm in size will dissolve before they reach the ocean surface, where the gas may be exchanged with the atmosphere. Because atomizers inject drops with sizes that belong in a statistical distribution (e.g., average size 2 mm with 0.2 mm standard deviation), injection at 600 m is recommended here to ensure that even the drops at the upper tail of the distribution (three standard deviations) have enough residence time in the seawater for complete dissolution of CO_2. The naturally occurring downward advection of the denser CO_2–H_2O mixture ensures the replenishment of the injection zone with seawater of lower CO_2 concentration.

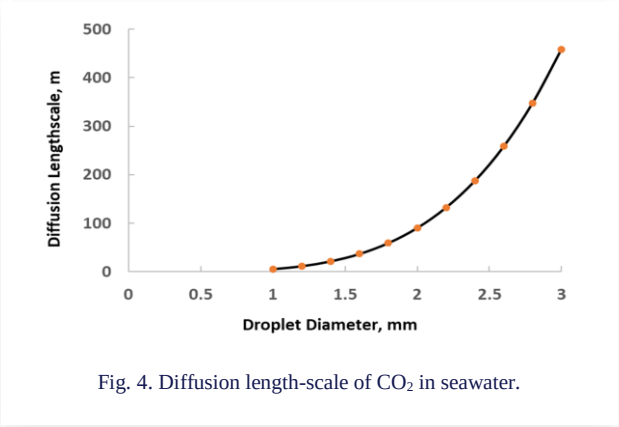

Fig. 4. Diffusion length-scale of CO_2 in seawater.

Alternatively, the CO_2 injection may be accomplished by a fleet of ships [33] that roam the ocean. In order to discharge all the CO_2, in their holds the ships will need to be furnished with compressors that will pressurize the CO_2 and inject it with a pressure higher than 6 MPa.

The monitoring of the CO_2 transportation pipelines and the injection sites is an essential part of the long-term carbon storage problem. Existing CO_2 pipelines in the USA are monitored bi-weekly by helicopters and injection/storage sites need to be continuously monitored by personnel. Such monitoring requires relatively small power consumption, but (because personnel is necessary) adds to the cost of storage. The IPCC report [2] estimates that the cost of monitoring is similar to that of transportation. However, monitoring optimization, – e.g. by partly using remote instrumentation facilities – significantly cuts this part of the CCS cost, as demonstrated in the existing CO_2 pipelines [37].

6. Total power for sequestration – the case of two Texan coal power plants

Calculations were performed for the total power needed for the capture, pressurization, transportation, and injection in the deep ocean of 90% of the yearly-averaged CO_2 emitted by two coal power plants in the ERCOT electrical grid of Texas. The first (case A) is the J. K. Spruce station, which is located outside the city of San Antonio at an elevation 198 m above sea level. The plant is composed of two units with a total power of 1 440 MW and uses subbituminous coal as its principal fuel. In 2021 this power plant generated 7 329 045 MWh and consumed total heat equivalent to 77.853×10^{12} MJ (73 213 439 MMBtu), indicating an average thermal efficiency of 33.89%. The plant emitted approximately 7.138×10^9 kg of CO_2 in the year 2021, or an average of 226.4 kg/s [56]. This power plant is 210 km from the Gulf of Mexico and 255 km from a location where the depth is at least 600 m. The Martin Lake power station in North Texas (case B) is composed of three units with a total rated power of 2 250 MW; it is located at an elevation of 98 m above sea level; and also uses subbituminous coal. In 2021 the Martin Lake power plant generated 13 179 510 MWh and consumed 151.317×10^{12} MJ (150 564 978 MMBtu) of heat with an average efficiency of 29.87%. The plant emitted approximately 14.680×10^9 kg of CO_2 or an average of 465.5 kg/s [57]. This power plant is located 350 km from the coast and 410 km from a location where the depth is at least 600 m. Regarding the transportation distances, it must be noted that the distance of the two power plants from the oil fields in the Permian Basin (for onshore storage) is slightly longer than their distance from the Gulf of Mexico storage sites.

It was stipulated that 90% of the emitted CO_2 – 204 kg/s for case A and 419 kg/s for case B – will be captured and transported to the storage locations. The hydrostatic pressure at 600 m is 6.033 MPa and the temperature is 277 K. As explained in section 4 it was also stipulated that, at the end of the pipeline, the CO_2 will be at supercritical pressure, that is its pressure will be at least 7.377 MPa. This is 1.344 MPa higher than the pressure at 600 m, which implies that the injection equipment will have enough pressure differential to operate. In all cases, common steel pipelines of schedule 30 were chosen for the transportation to withstand the high internal pressure.

Computations were performed to determine the pressure at the power plant that would enable the transportation and injection of CO_2. For the calculations, Eq. (4) was discretized and used in a finite-difference numerical scheme with the properties of CO_2 obtained from [36]. For case A it was determined that either an 18” (ID = 0.435 m) pipeline with initial pressure 14 MPa or a 20” (ID = 0.530 m) pipeline with initial pressure 9.2 MPa are sufficient for the CO_2 transport without an intermediate pressure station. For case B, which generates more CO_2 and is further from the injection region, it was determined that a 30” pipe (ID = 0.730 m) with initial pressure 11.4 MPa or a 28” pipe (ID =0.679 m) with 14.4 MPa initial pressure are sufficient to carry 90% of the emitted CO_2. The final choice of pipeline size will be determined by economic optimization, taking into account the pipeline cost and the cost of additional energy spent for the pressurization of the gas.

Table 1 shows some details for the total power and total annualized energy spent to operate the entire CCS system for the two cases. For the computations, the initial concentration of CO_2 in the flue gases is 15%. The efficiency of the separation process is 15%, slightly higher than the state-of-the-art facilities (12.8%), anticipating improvements following the current research efforts. The efficiency of the dual stage compressors is

82%, including the parasitic power for the intercooler. Based on the total CCS power in column 3, the fourth column shows the annual energy expenditure of the entire CCS system. The fifth column shows the net energy generated by the power plant. And the sixth column shows the yearly averaged thermal efficiency of the plant, when the energy for the CCS system is taken under consideration.

It is observed in Table 1 that the power for the separation (capture) of CO_2 from the flue gases is very significant, higher than that for the pressurization of the gas, even with the rather optimistic efficiency for separation. Also, that the entire CCS operations would consume close to one-third of the annual energy currently generated by the two power plants and that the thermal efficiency of these units drops by about 10 percentage points when the CCS energy is taken into account. This is in line with the range of estimates in [2], which does not include the injection process.

7. Cost of capture, transportation and storage

Viebahn and Chappin [58] conducted a bibliographical study and showed that the technical and research issues for the different processes that make up the CCS account for 69% of all the publications, while only 31% of the publications address the non-technical issues, which include estimates of the cost of the CCS processes, its effect on electricity prices, economic viability, the financing of the CCS projects in market-oriented economies, and political willingness.

Regarding any type of costs, one must always be cognizant of the fact that they are determined by labour and materials prices that rely on demand and supply considerations as well as the type of economy (market, centralized, regulatory, etc.). As a consequence, costs exhibit high variability [59] and, therefore, are laden with high uncertainty. Any economic analysis of the CCS projects is also laden with significantly higher uncertainty than the power and energy analyses of section 6, which are based on engineering principles and the state of technology. This is corroborated by a recent global assessment [60], which concluded that the costs of the onshore CO_2 transport and storage vary between \$4/ton and \$45/ton (variability of a factor of 11!). An assessment of the total CCS cost for five sites in the USA showed a similar range of variability with significantly higher costs – from \$18/ton to \$67/ton with a value as high as \$161/ton for a natural gas fueled power plant [61]. All of the CCS cost studies conclude that, since this is an evolving technology, further analysis with economic models is needed [2, 58, 59, 60, 61].

The principal costs for any CCS system are the pipeline (with the injection system at the end), the separation system, the compression system, and the cost of maintenance and monitoring. The capital cost of a pipeline in the USA market is made up of five separate costs:

1. Materials and Labour;
2. Rights of Way;
3. Trench construction;
4. Professional services (accounting, surveying, legal, etc.);
5. Terrain challenges (more expensive in rugged terrains). Offshore pipelines are almost twice as expensive as onshore pipelines and their construction cost increased by a factor of 4 since 1980 [59].

While the separation and compression capital costs are fairly well known and documented, the pipeline cost data for the USA market show significant variability with the principal variable being the length (in km) and size (in inches) of the pipe [59, 61, 62]. For this reason, the capital cost of the pipeline is treated as a parameter. Based on data from [60] and [62], for large (diameters larger than 10 inches) pipelines, this parameter varies in the range of \$50,000–\$120,000 per km and per inch.

In addition to the capital costs, the following are recurring annual expenses:

1. Monitoring (weekly or biweekly flights with helicopters, continuous instrument monitoring, education, and information of the urban populations near the pipeline, offshore injection region monitoring, etc.);
2. Maintenance and operational costs of the pipeline, the compression equipment, and the separation equipment;
3. The annual cost of the energy, which is generated by the power plants and diverted to the separation and compression systems.

The cost of the first two items is approximately 5% of the capital costs. For the fuel cost in item 3, the recent average cost of fuel (coal) was used – \$2.17 per MMBtu (\$2.07/GJ) [63] – as well as the average annual thermal efficiency of each power plant [56, 57]. This cost is the actual cost of the fuel to the utility corporation and is used here rather than the price of electricity.

A parameter that is crucial in market-oriented economies is the internal discount factor, r, of the pipeline corporations. The discount factor essentially takes into account the *time-value of money* by discounting future cash flows by a factor equal to $(1+r_d)^N$, where N is the year the cash flow is realized by the corporation [64, 65]. The discount rate, r_d, is higher during in-

Table 1. Power for the separation, transportation and injection of CO_2, annual energy consumed for CCS, net annual energy generated and power plant thermal efficiency.

	Separation MW	Transportation, Injection, MW	Total, MW	CCS Energy, GWh	Net Energy, GWh	Plant Efficiency, %
Case A, 18" pipe	162	103	265	2 325.6	5 003.4	24.5
Case A, 20" pipe	162	94	256	2 242.7	5 086.4	24.9
Case B, 28" pipe	333	214	548	4 796.6	8 382.9	19.9
Case B, 30" pipe	333	203	537	4 701.4	8 478.1	20.2

Table 2. Summary of CCS costs, cost per MWh and percentage price increase.

Discount rate, %	5	8	10	12	15
Case A, 18" pipe					
Ann. worth of capital	29 399 816	39 268 686	46 163 900	53 157 069	63 619 923
Additional cost	24 067 352	24 067 352	24 067 352	24 067 352	24 067 352
Cost of fuel for CCS	50 413 323	50 413 323	50 413 323	50 413 323	50 413 323
Cost per MWh	20.8	22.7	24.1	25.5	27.6
Price increase, %	61.1	66.9	70.9	75.0	81.2
Case B, 28" pipe					
Ann. worth of capital	63 958 878	85 428 464	100 428 905	115 642 443	138 404 232
Additional cost	52 358 180	52 358 180	52 358 180	52 358 180	52 358 180
Cost of fuel for CCS	118 910 540	118 910 540	118 910 540	118 910 540	118 910 540
Cost per MWh	28.1	30.6	32.4	34.2	36.9
Price increase, %	82.5	90.1	95.3	100.7	108.7

flationary times and is one of the dominant parameters for the appraisal of all long-term investments [66].

Using a lifetime for the CCS project of 30 years and a discount rate in the range of 5% to 15%, the capital cost for the construction of the entire CCS system was annualized using the annual worth, *AW*, value of the capital cost [67]:

$$AW = PV\left[\frac{r_d(1+r_d)^N}{(1+r_d)^{N+1}-1}\right], \quad (9)$$

where *PV* is the present (initial) cost of the investment and *N* is the lifetime of the project. The costs mentioned above in items 1–3 are added to the annual worth of the project to determine the total annualized cost.

Table 2 summarizes these results for two cases – using an 18" pipeline for the Spruce unit and a 28" pipeline for the Martin Lake unit. The costs in the table pertain to a unit cost for the construction of the pipeline of $70 000 per km and per inch; and 5% for the operations, maintenance, and monitoring cost of the pipeline. The percentage cost increase in the last lines has been calculated using the average selling price per MWh ($34/MWh) in the five-year period 2017–2021. In the absence of any subsidies for CCS, this cost is the minimum amount that will have to be added to the current average price of electricity for the utilities to recoup their investments.

The data of Table 2 are also shown graphically in Fig. 5. It is observed in Table 2 and Fig. 5 that the installation of a CCS unit that would remove 90% of the CO_2 generated in the two power plants would also add significantly to the cost of electricity generation. Changing the corporation discount rate from the low end of 5% to the high end of 15 %, would increase the cost of the entire CCS process by approximately 32% for both power plants. The lower part of the discount rates (5–8%) can only be achieved with government subsidies and loan guarantees – with such guarantees, bonds can be issued by the corporation at low interest. In the absence of loan guarantees or other governmental incentives, the investing corporations will use the upper range of the discount rates (12–15%) because they will have to issue their own bonds at a higher interest rate.

The other parameter that significantly affects the cost of transportation and storage is the unit cost of the pipeline, which is substantially higher in mountainous regions and offshore locations. Figure 6 shows the effect of this parameter on the cost

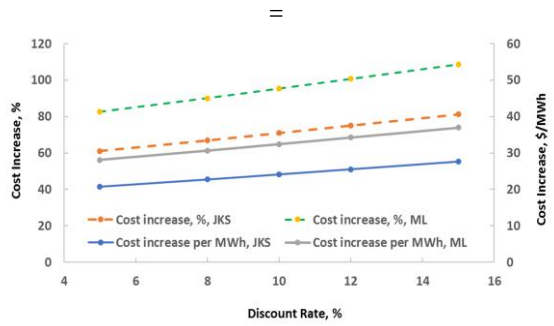

Fig. 5. The cost of carbon capture and storage for two power plants in Texas as a function of the discount rate.

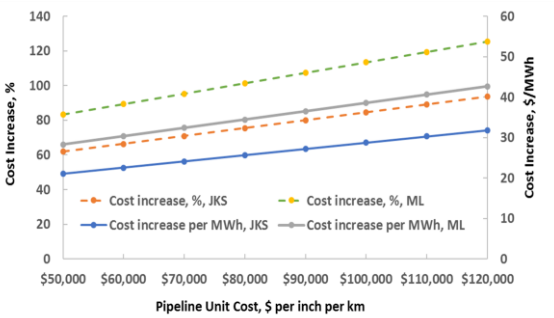

Fig. 6. The cost of carbon capture and storage for two power plants in Texas as a function of the unit cost of the pipeline.

increase as well as the fraction of this cost in relation to the average wholesale price of electricity, $34/MWh. It is observed in the data of Fig. 6 that doubling the unit price of the pipeline (e.g. from $50k to $100k) increases the total cost of the CCS process by 36%.

8. Conclusions

A holistic calculation of the energy required, and the associated cost for CCS entails calculations for four distinct processes: a) separation of CO_2 from the other flue gases; b) compression; c) transportation; and d) injection into the storage site. The separation of this gas from the flue gases requires mechanical work or a combination of high-temperature heat (which corresponds to significant equivalent work) and parasitic work. For the transportation part, the CO_2 should be in the dense supercritical state until it reaches the injection site. This implies that the gas must be compressed to states higher than 7.3 MPa at the expense of significant power. For the injection process, given the properties of this greenhouse gas, its dissolution with seawater at depths more than 600 m is very likely the most promising storage method at present.

Calculations were made for the power and annualized energy requirements as well as for the cost of the entire CCS for two power plants, located in Texas, USA. The CCS process for the Martin Lake unit would consume annually 31% of the total electricity generated by the plant. For the larger Spruce power plant, the CCS process would consume close to 36% of the annually generated electricity. The pipelines for the transportation of the compressed CO_2 to the storage sites, the separation unit, and the compression unit entail significant capital cost. Two parameters, the unit cost of the pipeline and the discount rate, have a significant influence on the total annualized cost of CCS. Doubling the unit prices for the pipeline installation increases by 36% the annual cost of the entire CCS system. Increasing the discount rate from 5% to 15% would increase this annualized cost of CCS by 32%.

Acknowledgements

This research was partly supported by the W.A. (Tex) Moncrief chair in Engineering at Technical Christian University.

References

[1] US-EPA. (2020). *Sources of Greenhouse Gas Emissions*. Report at: https://www.epa.gov/ghgemissions/sources-greenhouse-gas-emissions [accessed in June 2023].

[2] Metz, B., Davidson, O., de Coninck, H.C., Loos, M., & Meyer, L.A. (Eds.). (2007). *IPCC Special Report on Carbon Dioxide Capture and Storage*, Cambridge University Press, Cambridge, UK.

[3] Zevenhoven, R., Fagerlund, J., & Songok, J.K. (2011). CO_2 mineral sequestration: developments toward large-scale application. *GHG: Science and Technology*, 1(1), 48–57. doi: 10.1002/ghg3.7

[4] Rao, A., & Rubin, E. (2006). Identifying cost-effective CO2 control levels for amine-based CO2 capture systems. *Industrial and Engineering Chemistry Research*, 45(8), 2421–2429. doi: 10.1021/ie050603p

[5] Valenti, G., Bonalumi, D., & Macchi, E. (2009). Energy and exergy analyses for the carbon capture with the Chilled Ammonia Process (CAP). *Energy Procedia*, 1(1), 1959–1066. doi: 10.1016/j.egypro.2009.01.140

[6] Bonalumi, D., Lillia, S., & Valenti, G. (2019). Rate-based simulation and techno-economic analysis of coal-fired power plants with aqueous ammonia carbon capture. *Energy Conversion and Management*, 199, 111966. doi: 10.1016/j.enconman.2019.111966

[7] Weiland, R.H., Dingman, J.C., & Cronin, D.B. (1997). Heat Capacity of Aqueous Monoethanolamine, Diethanolamine, Nmethyldiethanolamine, and N-methyldiethanolamine-Based Blends with Carbon Dioxide. *Journal* of *Chemical and Engineering Data*, 42, 1004–1006. doi: 10.1021/je960314v

[8] Aliyon, K., Hajinezhad, A., & Mehrpooya, M. (2019) Energy assessment of coal-fired steam power plant, carbon capture, and carbon liquefaction process chain as a whole. *Energy Conversion and Management*, 199, 111994. doi: 10.1016/j.enconman.2019.111994

[9] Carapellucci, R., Di Battista, D., & Cipollone, R. (2019) The retrofitting of a coal-fired subcritical steam power plant for carbon dioxide capture: A comparison between MCFC-based active systems and conventional MEA. *Energy Conversion and Management*, 194, 124–139. doi: 10.1016/j.enconman.2019.04.077

[10] Rochelle, G., Chen, E., Freeman, S., Van Wagener, D., Xu, Q., & Voice, A. (2011). Aqueous piperazine as the new standard for CO2 capture technology. *Chemical Engineering Journal*, 171(3), 725–733. doi: 10.1016/j.cej.2011.02.011

[11] Li, X., Wang, S., & Chen, C. (2013). Experimental study of energy requirement of CO2 desorption from rich solvent. *Energy Procedia*, 37, 1836–1843. doi: 10.1016/j.egypro.2013.06.063

[12] Furcasa, F.E., Wanawan, P., Chacartegui, R., & Afzal, W. (2020). Sodium carbonate-based post combustion carbon capture utilising trona as main sorbent feed stock. *Energy Conversion and Management*, 208, 112484. doi: 10.1016/j.enconman.2020.112484

[13] Strube, R., Pellegrini, G., & Manfrida, G. (2011). The environmental impact of post-combustion CO2 capture with MEA, with aqueous ammonia, and with an aqueous ammonia–ethanol mixture for a coal-fired power plant. *Energy*, 36, 3763–3770. doi: 10.1016/j.energy.2010.12.060

[14] Lee, W.S., Lee, J.C., Oh, H.T., Baek, S.W., Oh, M., & Lee, C.H. (2017). Performance, economic and exergy analyses of carbon capture processes for a 300 MW class integrated gasification combined cycle power plant. *Energy*, 134, 731–742. 10.1016/j.energy.2017.06.059

[15] Kunze, C., Riedl, K., & Spliethoff, H. (2011). Structured exergy analysis of an integrated gasification combined cycle (IGCC) plant with carbon capture. *Energy*, 36, 1480–1487. doi: 10.1016/j.energy.2011.01.020

[16] Arabkhalaj, A., Ghassemi, H., & Markadeh, R.S. (2016). Thermodynamic evaluation of integrated gasification combined cycle: Comparison between high-ash and low-ash coals. *International Journal of Energy Research*, 40(12), 1638–1651. doi: 10.1002/er.3541

[17] Rosner, F., Qin, C., Rao, A., & Samuelsen S. (2019) Thermoeconomic analyses of concepts for increasing carbon capture in high-methane syngas integrated gasification combined cycle power plants. *Energy Conversion and Management*, 199, 112020. doi: 10.1016/j.enconman.2019.112020

[18] Petrakopoulou, F., Boyano, A., Cabrera, M., & Tsatsaronis, G. (2011). Exergoeconomic and exergoenvironmental analyses of a combined cycle power plant with chemical looping technology.

International Journal of Greenhouse Gas Control, 5(3), 475–482. doi: 10.1016/j.ijggc.2010.06.008

[19] Akinola, T.E., Bonilla Prado, P.L., & Wang, M. (2022). Experimental studies, molecular simulation and process modelling simulation of adsorption-based post-combustion carbon capture for power plants: A state-of-the-art review. *Applied Energy*, 317, 119156. doi: 10.1016/j.apenergy.2022.119156

[20] Zhang, X., He, X., & Gundersen, T. (2013). Post-combustion Carbon Capture with a Gas Separation Membrane: Parametric Study, Capture Cost, and Exergy Analysis. *Energy and Fuels*, 27(8), 3021798. doi: 10.1021/ef3021798

[21] Li, C., Guo, S., Ye, X., & Fu, W. (2019). Performance and thermoeconomics of solar-aided double-reheat coal-fired power systems with carbon capture. *Energy*, 177, 1–15. doi: 10.1016/j.energy.2019.04.058

[22] Carapellucci, R., Giordano, L., & Vaccarelli, M. (2015). Analysis of CO_2 post-combustion capture in coal-fired power plants integrated with renewable energies. *Energy Procedia*, 82, 350–357. doi: 10.1016/j.egypro.2015.11.801

[23] Saghafifar, M., & Gabra, S. (2020). A critical overview of solar assisted carbon capture systems: Is solar always the solution? *International Journal of Greenhouse Gas Control*, 92(10), 102852. doi: 10.1016/j.ijggc.2019.102852

[24] Michaelides, E. E. (2020). *Exergy and the Conversion of Energy.* Cambridge Univ. Press, Cambridge, UK.

[25] Paltsev, S., Morris, J., Kheshgi, H., & Herzog, H. (2021). Hard-to-Abate Sectors: The role of industrial carbon capture and storage (CCS) in emission mitigation. *Applied Energy*, 300, 117322. doi: 10.1016/j.apenergy.2021.117322

[26] Lee, H., Lee, J., & Koo, Y. (2022). Economic impacts of carbon capture and storage on the steel industry–A hybrid energy system model incorporating technological change. *Applied Energy*, 317, 119208. doi: 10.1016/j.apenergy.2022.119208

[27] Al Baroudi, H., Awoyomi, A., Patchigolla, K., Jonnalagadda, K., & Anthony, E.J. (2022). A review of large-scale CO_2 shipping and marine emissions management for carbon capture, utilisation and storage. *Applied Energy*, 287, 116510. doi: 10.1016/j.apenergy.2021.116510

[28] Michaelides, E.E. (2021). Thermodynamic Analysis and Power Requirements of CO_2 Capture, Transportation, and Storage in the Ocean. *Energy*, 230, 120804. doi: 10.1016/j.energy.2021.120804

[29] Zhai, H., Rubin, E.S., & Versteeg, P.L. (2011). Water use at pulverized coal power plants with post-combustion carbon capture and storage. *Environmental Science and Technology*, 45, 2479–2485. doi: 10.1021/es1034443

[30] Korbol, R., & Kaddour, A. (1995). Sleipner West CO_2 disposal: injection of removed CO_2 into the Utsira formation. *Energy Conversion and Management*, 36(6–9), 509–512. doi: 10.1016/0196-8904(95)00055-i

[31] Tanaka, S., Koide, H., & Sasagawa, A. (1995). Possibility of underground CO_2 sequestration in Japan. *Energy Conversion and Management*, 36(6–9), 527–530. doi: 10.1016/0196-8904(95)00059-M

[32] Kharaka, Y.K., Cole, D.R., Hovorka, S.D., Gunter, W.D., Knauss, K.G., & Freifeld B.M. (2006). Gas-water-rock interactions in Frio formation following CO_2 injection: Implications for the storage of greenhouse gases in sedimentary basins. *Geology*, 34(7), 577–580. doi: 10.1130/G22357.1

[33] Ozaki, M., Minamiura, J., Kitajima, Y., Mizokami, S., Takeuchi, K., & Hatakenka, K. (2001). CO_2 ocean sequestration by moving ships. *Journal of Marine Science and Technology*, 6(2), 51–58. doi: 10.1007/s773-001-8375-8

[34] Caldeira, K., & Wickett, M.E. (2003). Anthropogenic carbon and ocean pH. *Nature*, 425, 365–365. doi: 10.1038/425365a

[35] Caldeira, K., & Wickett, M.E. (2005). Ocean model predictions of chemistry changes from carbon dioxide emissions to the atmosphere and ocean. *Journal of Geophysical Research–Oceans*, 110(C9), C09S04. doi: 10.1029/2004JC002671

[36] REFPROP. (2013). *Reference Thermodynamic and Fluid Transport Properties.* National Institute of Standards and Technology, Boulder, Colorado.

[37] Wallace, M., Goudarzi, L., Callahan, K., & Wallace, R. (2015). *A Review of the CO_2 Pipeline Infrastructure in the U.S.* DOE/NETL Report-2014/1681

[38] Philips, P. (1912). The viscosity of carbon dioxide. *Proceedings of the Royal Society*, 87, 48–61.

[39] https://www.engineeringtoolbox.com/carbon-dioxide-dynamic-kinematic-viscosity-temperature-pressure-d_2074.html [accessed Feb. 2, 2023].

[40] Li, Y.H., & Tsui, T.F. (1971). The Solubility of CO_2 in Water and Sea Water. *Journal of Geophysical Research*, 76(18), 4203–4207. doi: 10.1029/JC076i018p04203

[41] Song, Y., Chen, B., Nishio, B., & Akai, B. (2005). The study on density change of carbon dioxide seawater solution at high pressure and low temperature, *Energy*, 30(11–12), 2298–2307. doi: 10.1016/j.energy.2003.10.022

[42] Hamond, H.F., & Fechner-Levy, E.J. (2000). *Chemical Fate and Transport in the Environment.* Academic Press, San Diego.

[43] Karmakar, S., Kolar, A.K. (2013). Thermodynamic analysis of high-ash coal-fired power plant with carbon dioxide capture. *International Journal of Energy Research*; 37(6), 522–34. doi: 10.1002/er.1931

[44] Davison, J.E. (2005). CO_2 capture and storage and the IEA Greenhouse Gas R&D Programme. *Workshop on CO_2 issues*, Middelfart, Denmark.

[45] Nessi, P., Papadopoulos, A., Kazepidis, P., Polichroniadis, A., Nitourou G., Voutetakis, S., & Seferlis, P. (2022). Pilot Scale Assessment of a Novel Phase-change Solvent for Energy Efficient Post-combustion CO_2 Capture, *Journal of Environmental Management*, 317(C), 115489. doi: 10.1016/j.jenvman.2022.115489

[46] Michaelides, E.E., Crowe, C.T., & Schwarzkopf, J.D. (Eds.) (2017). *Multiphase Flow Handbook* (2nd ed.). CRC Press, Boca Raton.

[47] Munson, B. R., Young, D. F., Okiishi, T. H., & Huwbsch, W. W. (2009). *Fundamentals of Fluid Mechanics*. Wiley.

[48] European Commission Report: https://joint-research-centre.ec.europa.eu/jrc-news/global-CO2-emissions-rebound-2021-after-temporary-reduction-during-covid19-lockdown-2022-10-14_en [accessed June 3, 2023].

[49] Hovorka, S.D., Meckel, T.A., & Trevino, R.H. (2013). Monitoring a large-volume injection at Cranfield, Mississippi—Project design and recommendations. *International Journal of Greenhouse Gas Control*, 18, 345–360. doi: 10.1016/j.ijggc.2013.03.021

[50] EIA. (2009). *Sleipner Project – CO_2 Capture and Storage*. EIA Greenhouse Gas R&D Programme Report.

[51] McBride-Wright, M., Maitland, G.C., & Trusler, J.P.M. (2015). Viscosity and Density of Aqueous Solutions of Carbon Dioxide at Temperatures from 274 to 449 K and at Pressures up to 100 MPa. *Journal of Chemical Engineering Data*, 60(1), 171−180. doi: 10.1021/je5009125

[52] Fritching, U., & Li, X.G. (2017). Spray Systems. In *Multiphase Flow Handbook* (2nd ed.). Michaelides, E.E., Crowe, C.T., & Schwarzkopf, J.D. (Eds.). pp. 1059−1090, CRC Press, Boca Raton.

[53] Michaelides, E.E. (2006). *Particles, Bubbles and Drops, Their motion, Heat and Mass Transfer*. World Scientific, New Jersey.

[54] Cadogan, S.P., Maitland, G.C., & Trusler, .J.P.M. (2015). Diffusion Coefficients of CO_2 and N_2 in Water at Temperatures between 298.15 K and 423.15 K at Pressures up to 45 MPa. *Journal of Chemical Engineering Data*, 59(2), 519−525. doi: 10.1021/je401008s

[55] Liu, Q., Endo, H., Fukuda, K., Shibahara, M., & Zhang, P. (2016). Experimental Study on Solution and Diffusion Process of Single Carbon Dioxide Bubble in Seawater. *Mechanical Engineering Journal*, 3(2), 1–9. DOI: 10.1299/mej.16-00269

[56] https://www.eia.gov/electricity/data/browser/#/plant/7097 [accessed in June 2023].

[57] https://www.eia.gov/electricity/data/browser/#/plant/6146 [accessed in June 2023].

[58] Viebahn, P., & Chappin, E.J.L. (2018). Scrutinising the Gap between the Expected and Actual Deployment of Carbon Capture and Storage—A Bibliometric Analysis. *Energies*, 11(9), 2319. DOI: 10.3390/en11092319

[59] Smith, C.E. (2016). Natural gas pipeline profits, construction both up. *Oil and Gas Journal*, September 5.

[60] Smith, E., Morris, J., Kheshgi, H., Teletzke, G., Herzog, H., & Paltsev, S. (2021). The cost of CO_2 transport and storage in global integrated assessment modelling. *International Journal of. Greenhouse Gas Control*, 109(2**),** 103367. doi: 10.1016/j.ijggc.2021.103367

[61] McKaskle, R. (2021). *Screening-Level Cost Estimates for CO_2 Capture and Transportation*. DOE report, DOE- FE0029381−11.

[62] How is the cost per mile determined? https://hanginghco.com/natural-gaspipeline-construction-cost-per-mile/last [accessed in June 2023].

[63] https://www.eia.gov/electricity/data.php [accessed July 10, 2023].

[64] Sullivan, W.G., Wicks, E.M., & Luxhoj, J.T. (2023). *Engineering Economy* (12^{th} ed.). Pearson, New Jersey.

[65] Park, C.S. (2007). *Contemporary Engineering Economics* (4^{th} ed.). Pearson, New Jersey.

[66] Götze, U., Northcott, D., & Schuster, P. (2015). *Investment Appraisal: Methods and Models* (2^{nd} ed.). Springer, Heidelberg.

[67] Michaelides, E. E. (2018). *Energy, the Environment and Sustainability*. CRC Press, Boca Raton.